Artificial Intelligence in Agriculture 5 (2021) 185–195

Contents lists available at ScienceDirect

Artificial Intelligence in Agriculture

journal homepage: http://www.keaipublishing.com/en/journals/artificial-intelligence-in-agriculture/

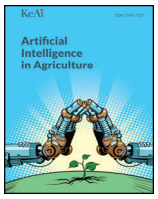

Modeling the energy gain reduction due to shadow in flat-plate solar collectors; Application of artificial intelligence

Morteza Taki *, Rouhollah Farhadi

Department of Agricultural Machinery and Mechanization Engineering, Agricultural Sciences and Natural Resources University of Khuzestan, P.O. Box: 6341773637, Mollasani, Iran

ARTICLE INFO

Article history:
Received 13 May 2021
Received in revised form 10 July 2021
Accepted 25 August 2021
Available online 24 September 2021

Keywords:
Multilayer perceptron
Optimization
Energy
Sensitivity analysis

ABSTRACT

Energy lost due to shadow in the absorber plate of solar collectors can decrease the solar energy gain. In some studies, mathematical modeling was applied for calculating the energy gain reduction due to shadow in flat-plate solar collectors. In this study, ANN method was developed for modeling the energy gain reduction. Multilayer Perceptron (MLP) with one hidden layer and a range of neurons (5–30) by two training algorithms (LM and BR) and tangent sigmoid activation function (TanSig) were used by help of K-fold cross validation method. In the first section, six set of solar collector dimensions were used (1×1; 1×1.5; 1×2; 1.5×1.5; 1.5×2 and 2×2). In the second section all the range of dimensions were used as the inputs. The results of the first section showed that MLP with BR training algorithm can predict the energy gain reduction with minimum MAPE and RMSE in all the categories. The best results related to (1.5×1.5) dimension that achieved a MAPE of 0.15 ± 0.09% and RMASE of 4.42 ± 2.43 KJm^{-2} $year^{-1}$, respectively. The results of the second section indicated that BR is a better training algorithm than LM. The MAPE and R^2 factors for the best topology (5-27-1) were 0.0610 ± 0.0051% and 0.9999 ± 0.0001, respectively. The results of the sensitivity analysis showed that height has the biggest impact on total energy gain reduction due to shadow in flat-plate solar collectors. Finally, the results of this study indicated that by using ANN and decrease the energy lost, the efficiency of solar collectors can be increased in all applications such as industry and agriculture.

1. Introduction

Fossil fuels are not good sources for future energy supply because of limited resources, price fluctuations, environmental pollution, etc. (Fadaei et al., 2018). So, the human should find another replacement resource for energy generation. Solar energy can be continuously used by humans because of its cleanliness and abundance (Kalani et al., 2017). Between all the solar energy systems, solar collectors and especially flat-plate solar collectors are widely used by people as a cheap and inexpensive energy system for warming air and water (Al-Waeli et al., 2019). They are simpler to manufacture, they receive direct and indirect radiation and do not require solar trackers (Kalogirou, 2014). Solar collectors can be used in agriculture and industry. In agriculture, the greenhouse extended the use of solar energy from post-harvest to crop-production (Taki et al., 2018a). Today greenhouses are ubiquitous with a huge variety of designs providing a wide range of modified climates for plant growth. Solar energy also finds use in agriculture in solar water pumping for irrigation and in the desalination of brackish water (Farhadi and Taki, 2020). Solar cooking has taken the use of solar energy in the food production chain directly to the end-user. Broader industrial uses of solar energy have also tended to be linked to food and beverage production because the temperatures required can be satisfied readily in many climates by a well-designed solar thermal system. Non-agricultural technologies such as solar furnaces have considerable potential but have had limited practical use to-date (Taki et al., 2018b).

Flat-plate solar collectors typically have one or two layers of transparent glass on the absorber plate to reduce losses due to convective air flow (Duffie and Beckman, 2013). This transparent glass is located at a distance from the absorbent plate. Increasing this distance reduces convective losses. But, it creates shadows on the absorbent plate and reduces the absorption radiation of the sun and ultimately decreases the performance (Farhadi and Taki, 2020). This distance is suggested in some researches between 4 and 5 cm (Nahar and Garg, 1980). The best distance can be calculated by shadow estimation, which has been done in previous research by Farhadi and Taki (2020). In this study, the authors decided to introduce a fast and accurate method for calculating the energy gain reduction in flat-plate solar collectors due to shadow by using Artificial Intelligence (AI).

AI with some simplistic modeling of real neural systems, is widely used for solving various science problems. The scope of AI application

* Corresponding author.
E-mail address: mtaki@asnrukh.ac.ir (M. Taki).

https://doi.org/10.1016/j.aiia.2021.08.002

is so wide (Taki et al., 2018a). It covers classification to applications, such as interpolation, estimation, detection, etc. (Rohani et al., 2019; Amini et al., 2020). Maybe the most important advantage of this method is its high speed and acceptable accuracy than traditional mathematical methods (Alonso et al., 2012). Nowadays various models of AI including Artificial Neural Network (ANN), Support Vector Machine (SVM), Adaptive Neuro Fuzzy Inference System (ANFIS) and …, are used in most aspects of engineering science (Elsheikh et al., 2019). ANNs are dynamic systems that transmit empirical knowledge or the law behind the data into a network structure. These systems learn general rules based on the calculations of the numerical data or examples and are intelligent systems (Alonso et al., 2012). The scientists predict that ANN will be used in the future in all aspect of human life because of its ability to modeling the linear and nonlinear systems as well as the need for no preconditions (Rohani et al., 2018).

Application of AI in solar energy systems in some studies was evaluated. Table 1 indicates some of the recent researches on different types of solar energy systems using AI. In a research, ANN with three hidden layers was used for evaluation the output of Photovoltaic Thermal (PV/T) air collector (Dimri et al., 2019). In this study, ANN applied for prediction the output fluctuating (thermal and electrical energy gain and also overall thermal energy and exergy gain). The results indicated that the traditional techniques were complex compared to ANN method. The ANN model based on the three inputs (global, diffuse and ambient solar radiation) showed a reasonable prediction accuracy (MSE = 0.086) and (R = 0.9997). Some other researchers used different types of ANN models for PV/T systems and reported reasonable prediction accuracy than traditional methods (Jia et al., 2019). In another study, ANN was used to predict the output in parabolic trough solar collector tube (Heng et al., 2019). The results showed that ANN is fast and accurate prediction method for calculating the exit temperature in parabolic trough solar collectors. Some others studies showed the ANN method is accurate, fast and reliable (Rohani et al., 2019; Al-Waeli et al., 2019; Amini et al., 2020; Rohani et al., 2018; Taki et al., 2018b).

1.1. Scope, innovations and structure

Based on the above literatures and Table 1, this research attempts to apply ANN for calculating the energy gain reduction due to shadow in flat-plate solar collectors. This study considers all the latitudes and the dimensions of the flat plate solar collectors. So, the results can be useful for all the solar energy engineers in the world. Main goals of this research are: Application of ANN-MLP model using two training algorithms include Levenberg Marquardt (LM) and Bayesian Regularization (BR), Application of K-fold cross validation method for increasing the accuracy and reliability of the results and sensitivity analysis for indicating the share of the inputs on output changing.

It is also the first attempt to investigate the application of ANN for calculating the energy gain reduction in one of the solar energy systems. In this study, Section 2 shows the methodology of the article – focusing

Table 1
Literature review of ANN application in solar energy systems.

No	Solar energy system	Authors	Model
1	Solar collectors	Benli, 2013	FFNN
		Hamdan et al., 2016	ANN model using resilient BP learning algorithm
		Kalogirou, 2006	ANN
		Heng et al., 2019	ANN
		Tomy et al., 2016	ANN
		Loni et al., 2018	ANN (group method of data handling ANN)
2	Solar air heaters	Esen et al., 2009	ANN-MLP and WNN models
		Ghritlahre and Prasad, 2017	ANN with four different training algorithms
		Aidinlou and Nikbakht, 2017	ANN
		Varol et al., 2010	ANN, SVM and ANFIS
		Ghritlahre and Prasad, 2018	ANN with LM training algorithm
		Saravanakumar et al., 2013	ANN
3	Solar water heaters	Kalogirou et al., 1999	ANN with three different activation functions in hidden layer
		Kalogirou and Panteliou, 2000	ANN with three different activation functions in hidden layer
		Souliotis et al., 2009	ANN integrated with TRNSYS
		Jahangiri Mamouri and Bénard, 2018	ANN
		Assari et al., 2018	ANN
		Mostafaeipour et al., 2017	ANN
4	Solar assisted heat pumps	Mohanraj et al., 2008	A feed forward network with LM training algorithm
		Kai et al., 2009	ANN-RBF
		Kumar et al., 2016	ANN integrated with GA
		Esen et al., 2017	ANN and ANFIS
		Mohanraj et al., 2018	ANN
		Hematian et al., 2021	Modeling
5	Photovoltaic/thermal (PV/T) systems	Nemati et al., 2016	ANN
		Kalani et al., 2017	ANN (MLP and RBF)-ANFIS
		Elsheikh and Abd Elaziz, 2018	PSO
		Mellit et al., 2013	ANN with Hyperbolic tangent sigmoid for hidden layer
		Graditi et al., 2016	ANN
		Khatib et al., 2018	ANN
6	Solar cookers and solar stills	Kurt et al., 2008	ANN-FFNN based on BP algorithm
		Nkhonjera et al., 2017	ANN-MLP
		Joshi and Jani, 2015	ANN
		Herez et al., 2018	ANN
		Mashaly and Alazba, 2015	ANN with tree different training functions
		Rai et al., 2005	ANN with sigmoid and hyperbolic transfer function tangent transfer functions
7	Solar dryers and solar greenhouses	Tripathy and Kumar, 2009	ANN with five different training algorithms
		Çakmak and Yıldız, 2011	ANN-FFNN
		Taki et al., 2018b	ANN (MLP-RBF)-SVM
		Taki et al., 2016	ANN-MLP
		Castañeda-Miranda and Castaño, 2017	ANN with LM training algorithm
		Fourati, 2014	ANN with an Elman structure

Table 2
Some statistical parameters of data used in each category in this study.

Dimensions	Average (KJm^{-2} $year^{-1}$)	Standard deviation (KJm^{-2} $year^{-1}$)	Kurtosis	skewness
1×1	1902	445	0.11	−0.74
1×1.5	1972	427	0.11	−0.80
1×2	2009	417	0.10	−0.82
1.5×1.5	2013	413	0.17	−0.84
1.5×2	2051	403	0.14	−0.86
2×2	2073	396	0.15	−0.88

Table 3
Total inputs of ANN model for the second section in this study.

Length of collector (m)	Width of collector (m)	Height of collector (m)	Tilt angle	Latitude
0.5–2.5	0.5–2.5	0.01–0.2	0.01–80°	0.01–65°

on data, ANN method and statistical parameters. Section 3 report the results of ANN method with real data and also presents a guideline of future researches. The last section is the overall conclusions and recommendations of this study.

2. Materials and methods

2.1. Data collection

Flat-plate solar collectors are getting more attention every day due to their simplicity and reasonable price. The absorber plate in these collectors is enclosed to reduce heat loss with a transparent glass above and heat-insulated walls from around. But often shadow covers some part of absorber plate, which reduces the performance. In the previous study (Farhadi and Taki, 2020), a mathematical model was used to determine the factors affecting shadow formation (latitude, tilt angle and collector dimensions). The results showed that height and width had the highest effect and latitude had the least share in shadow formation. In the present study, the authors try to estimate the energy loss due to shadow in flat-plate solar collectors using AI. The required data was extracted from the study of Farhadi and Taki (2020). In the first step, the data were categorized based on the dimensions. So, based on the Table 2, six categories were selected based on the popular and practical purpose.

In the second section, all the data were used for analysis (Table 3). In this section, more than 8000 rows of data were extracted and prepared for ANN analysis.

2.2. Artificial neural network

The MLP neural network will generate the output vector (z^q) for each q ($q = 1.2.3…Q$) by receiving the input vector (x^q). The goal is to adopt the correct network parameters to achieve the actual output that is close to the desired output with high accuracy (Ranjbar et al., 2013). In this study, basic Back Propagation (BP) algorithm was used for learning the network. Initially, the data were randomly divided into two groups: training set (60% of total data) and test set (40% of total data). If this segmentation does not produce the desired results, this step can be repeated again. Before applying the raw data, the data must be normalized, because the learning algorithm with the raw data cannot produce the suitable results. When using the Tangent Sigmoid (TanSig) activation function, the best data conversion range is [−1 to +1]. Linear normalization was used to convert the data (Rohani et al., 2018):

$$x_n = \frac{x - x_{min}}{x_{max} - x_{min}} \times (r_{max} - r_{min}) + r_{min} \quad (1)$$

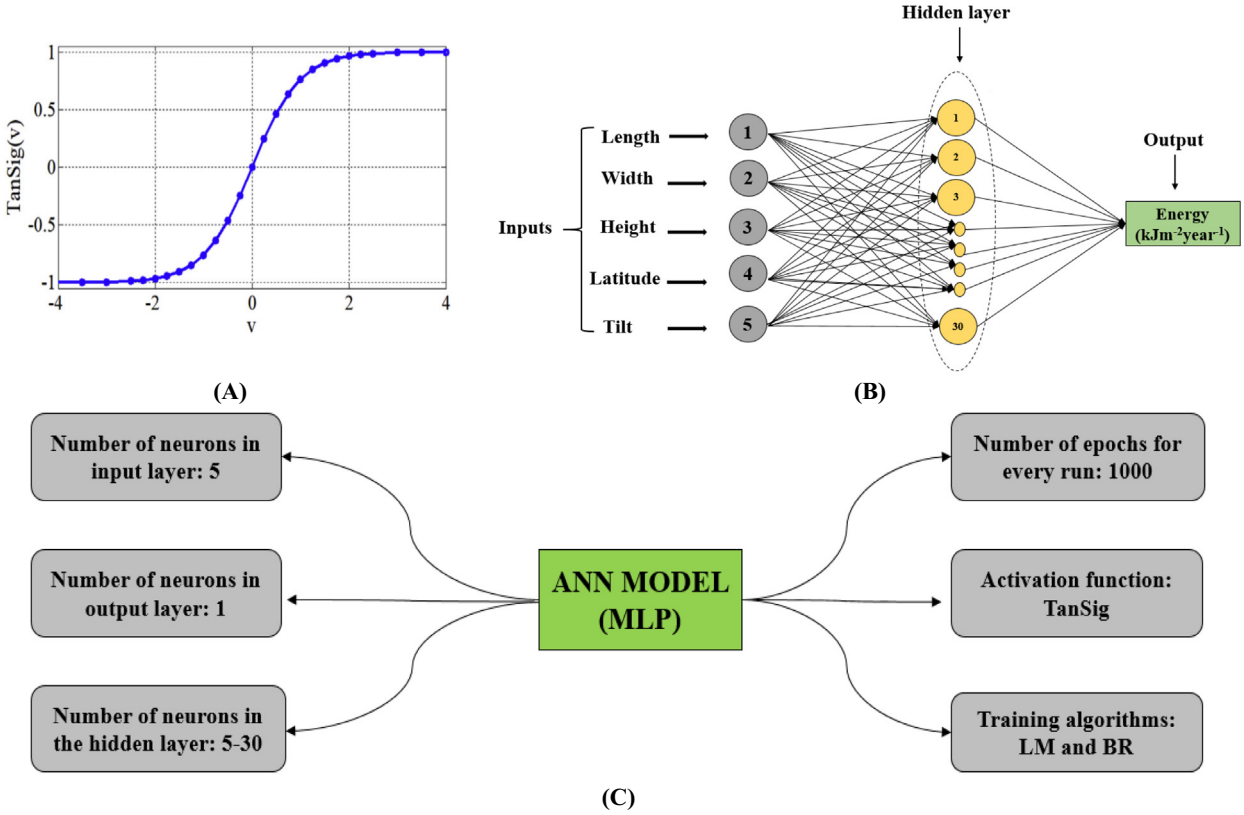

Fig. 1. A: TanSig activation function (Yilmaz et al., 2019); **B**: Overall structure of MLP applied for modeling; **C**: The organization of MLP structure in this study.

where, x is the raw and x_n is normalized data, x_{max} and x_{min} are the maximum and minimum values of the primary data, and r_{max} and r_{min} are the upper and lower limits of data ranges, respectively.

In this study two training algorithms were used: Levenberg Marquardt (LM) and Bayesian regularization (BR). Due to the high speed of network response and avoidance of complexity, a single layer network was used in this study (Ranjbar et al., 2013). The number of neurons in hidden layer increased as the results improved and was considered constant after the error increased. In this study, the maximum number of neurons in hidden layer was 30. Fig. 1. shows the overall structure of MLP model with all the components in this study.

2.3. K-fold cross validation

In this research, K-fold cross validation method was used for increasing the confidence of ANN outputs. In this method, the validation data are divided into different categories of K, based on their type and number, and are evaluated by each algorithm. In each step, K subsets is used for accreditation and the others (K-1) are applied for training (Rodriguez et al., 2010). This K procedure is repeated and all data are used for training and validation (in this study, K = 5). Finally, the average results are validated as a final estimation. Application of K-fold as a stochastic subdivision in this method can increase the distribution in the ANN process and makes the neural network normally used as a practical method with acceptable results (Taki et al., 2018a). In some studies, this method was used and the authors reported that the results can be used in the experimental sections because of reliability (Taki et al., 2018b; Rohani et al., 2019; Amini et al., 2020).

In order to evaluate the performance of ANN-MLP model, Mean Absolute Percentage Error (MAPE), coefficient of determination (R^2), Root Mean Square Error (RMSE) and Efficiency Factor (EF) were used (Rohani et al., 2019):

$$\mathrm{MAPE} = \frac{1}{n}\sum_{j=1}^{n}\left|\frac{d_j - p_i}{d_j}\right|.100 \tag{2}$$

$$R^2 = \frac{\left(\sum_{j=1}^{n}\left(d_j-\overline{d}\right)\left(p_j-\overline{p}\right)\right)^2}{\sum_{j=1}^{n}\left(d_j-\overline{d}\right)^2\sum_{j=1}^{n}\left(p_j-\overline{p}\right)^2} \tag{3}$$

$$\mathrm{RMSE} = \sqrt{\frac{\sum_{j=1}^{n}\left(d_j-p_j\right)^2}{n}} \tag{4}$$

$$\mathrm{EF} = \frac{\sum_{j=1}^{n}\left(d_j-\overline{d}\right)^2 - \sum_{j=1}^{n}\left(p_j-d_j\right)^2}{\sum_{j=1}^{n}\left(d_j-\overline{d}\right)^2} \tag{5}$$

Where d_j is the *jth* component of the actual output for the *jth* pattern; p_j is the component of the predicted output produced by the network for the *jth* pattern; $\overline{d}$ and $\overline{p}$ are the average of the whole actual and predicted output and n is the number of variable outputs. A model with the smallest RMSE, MAPE and largest EF is considered to be the best. Also, MATLAB software 2018a was used to analyze neural network and regression methods. Fig. 2 shows the whole procedure of methodology in this study.

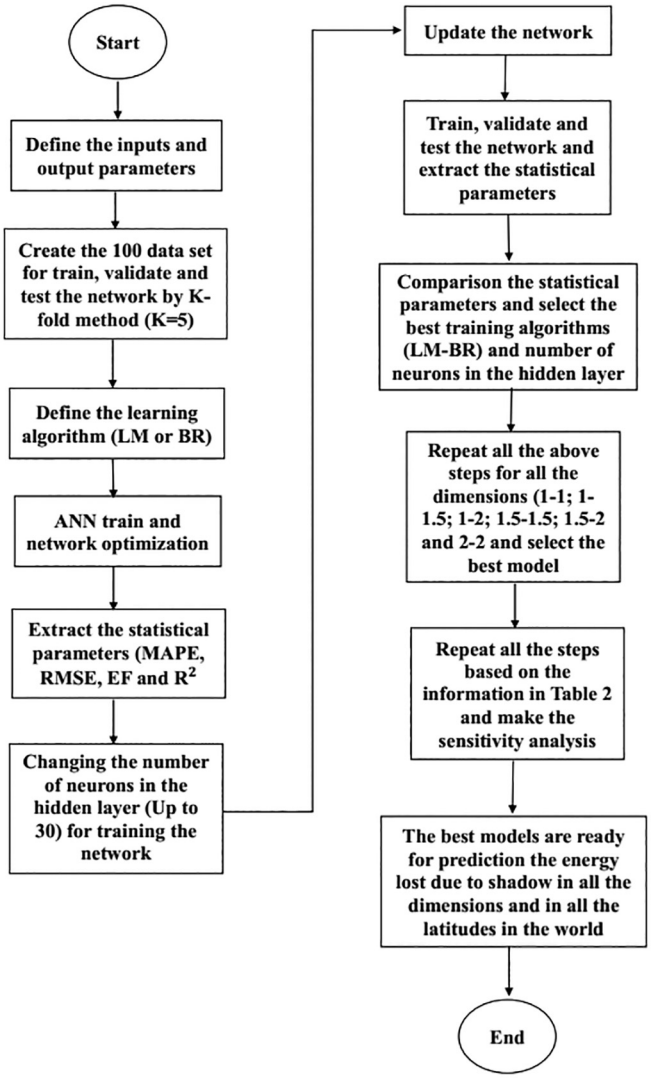

Fig. 2. Methodology process for ANN modeling in this study as a flowchart.

3. Results and discussion

3.1. The best algorithm for MLP

In this study two training algorithms were used for MLP model (LM and BR). The Levenberg-Marquardt (LM) algorithm is a method for finding the minimum of a multivariate nonlinear function that has become a standard method for solving the least squares problem in nonlinear functions (Najafi et al., 2009). Bayesian Regularization (BR) algorithm is more robust than other traditional algorithms such as standard back-propagation and can decrease the need for long cross-validation. BR is a mathematical process that change a nonlinear regression into a well-posed statistical problem in the manner of a ridge regression. The advantage of BR is that this method is robust and the validation process, such as back propagation, is unnecessary (Amini et al., 2020). For transfer function, TanSig was used. This type of transfer function is very popular and many researchers applied this method in ANN studies (Taki et al., 2018b; Ranjbar et al., 2013; Rohani et al., 2019). In the first section, six types of data based on the collector dimensions were used for modeling. Two training algorithms and several number of neurons in hidden layer (1,2, 3….,30) were used for ANN process. Fig. 3. shows the results of MLP model with two training algorithm (LM-BR) to predict the energy lost due to shadow for different dimensions of flat-plate solar collectors. As the results show, the BR algorithm has the better performance than LM in all the six categories. The MAPE factor was varied between 0.119%–0.267% and 0.879%–1.87%, for BR and LM algorithms, respectively.

The results show that the BR algorithm can make accurate output data and based on the K-fold cross validation, this model (MLP-BR) can use in real experimental applications. So for other analysis, the BR

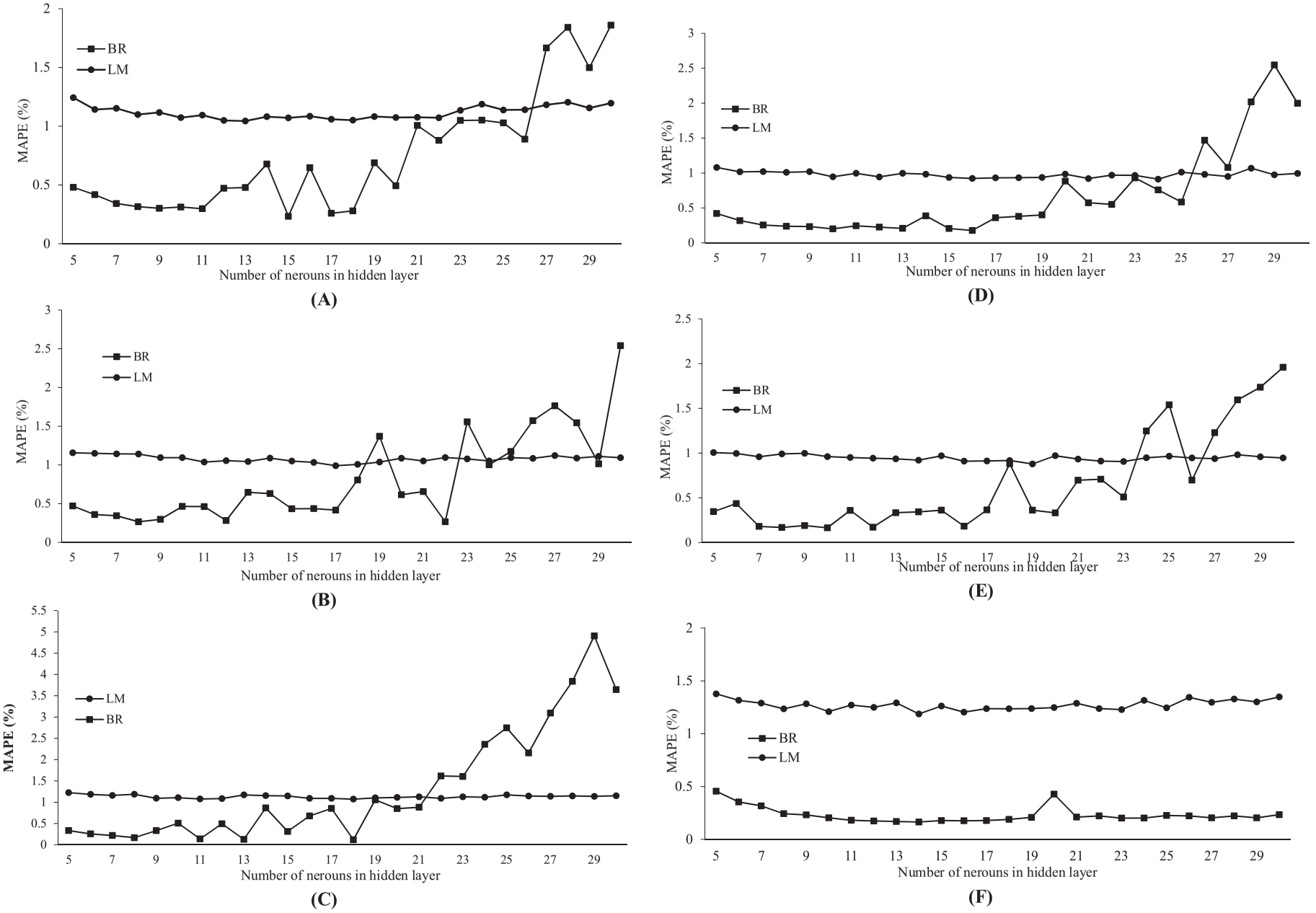

Fig. 3. The results of MLP model with two training algorithm (LM-BR) to predict the energy lost due to shadow for different dimensions of flat-plate solar collectors, A: (1-1), B: (1-1.5), C: (1-2), D: (1.5-1.5), E: (1.5-2), F: (2-2).

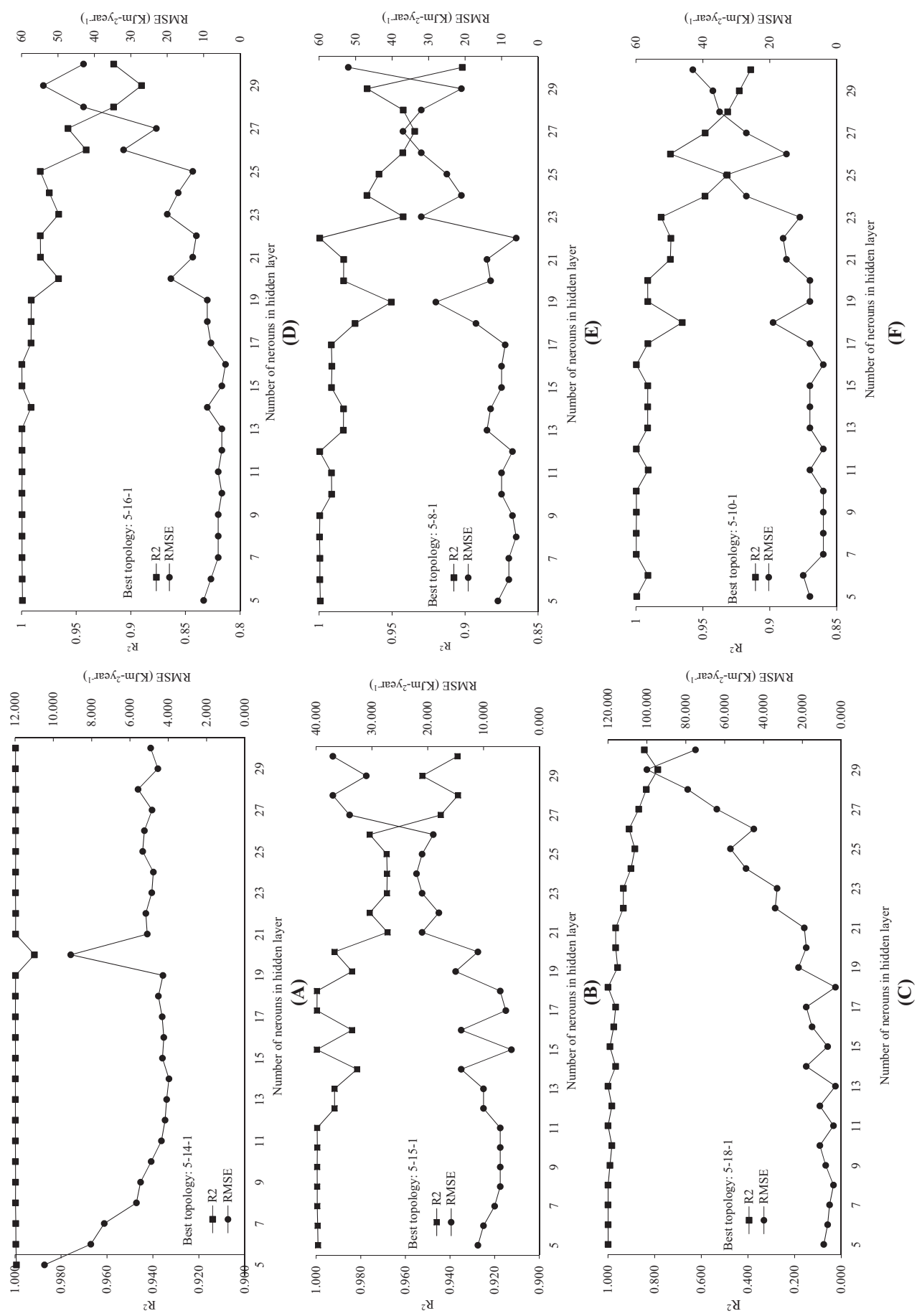

Fig. 4. The results of MLP model with BR training algorithm (MLP-BR) or the best topologies, to predict the energy lost due to shadow for different dimensions of flat-plate solar collectors, A: (1-1), B: (1-1.5), C: (1-2), D: (1.5-1.5), E: (1.5-2), F: (2-2).

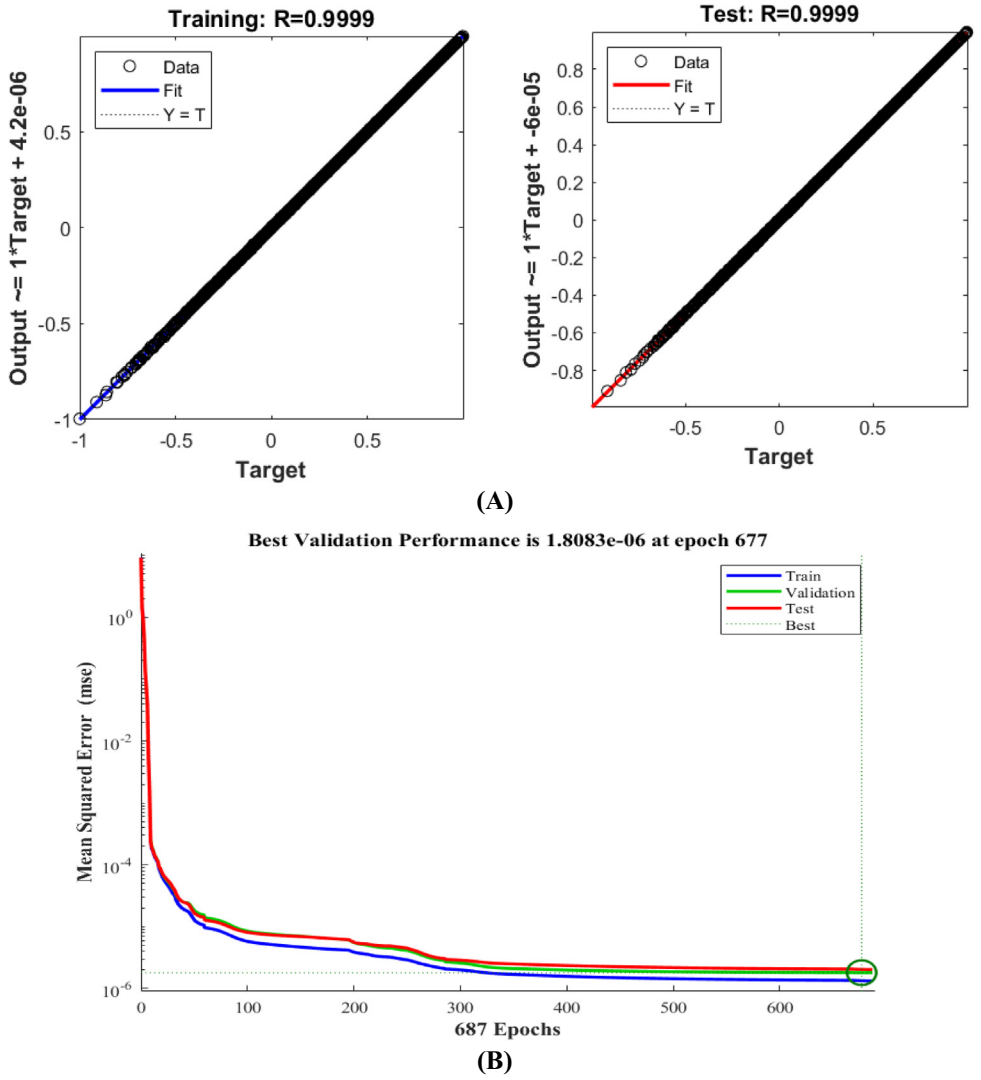

Fig. 5. A: The agreement between the actual and predicted data by MLP model with BR training algorithm; **B:** The convergence diagram of MLP-BR model to predict the energy lost due to shadow in flat-plate solar collectors.

was used. Fig. 4 shows the RMSE and EF factors for the best neuron in the hidden layer by BR algorithm. The results of Fig. 5 show that for the six dimensions (1×1; 1×1.5; 1×2; 1.5×1.5; 1.5×2 and 2×2) the best topologies are: 5-14-1; 5-15-1; 5-8-1; 5-18-1; 5-16-1; 5-10-1, respectively. The lowest RMSE is related to (1.5×1.5) dimension. Also this dimension has the highest EF (0.9999). The results of this figure show that the number of neurons in the hidden layer can play an important role in the final performance but the higher number of neurons in the hidden layer is not always a reason for increasing the efficiency and accuracy of the neural network model. Table 4 shows the overall performance of MLP model for the best neurons in the hidden layer by BR algorithm in the train and test phases. The results of Table 5 show that MLP model with proposed structure can predict the energy lost due to shadow for all the dimensions with high accuracy. For flat-plate solar collectors with (1.5×1.5) dimension, MLP model can use with higher performance than other dimensions.

Table 4
The statistical parameters of the of MLP-BR model with optimal neuron in hidden layer to predict the energy lost due to shadow in flat-plate solar collectors.

Dimensions	Topology	Train				Test			
		RMSE (KJm^{-2} $year^{-1}$) ($\bar{x}$±SD)	MAPE % ($\bar{x}$±SD)	EF (−) ($\bar{x}$±SD)	R^2 (−) ($\bar{x}$±SD)	RMSE (KJm^{-2} $year^{-1}$) ($\bar{x}$±SD)	MAPE % ($\bar{x}$±SD)	EF (−) ($\bar{x}$±SD)	R^2 (−) ($\bar{x}$±SD)
1×1	5–14-1	2.97 ± 2.5	0.15 ± 0.12	0.99 ± 0.01	0.99 ± 0.01	4.48 ± 2.9	0.18 ± 0.11	0.99 ± 0.01	0.99 ± 0.01
1×1.5	5–15-1	4.08 ± 4.4	0.18 ± 0.19	0.99 ± 0.01	0.99 ± 0.01	6.84 ± 5.6	0.27 ± 0.23	0.99 ± 0.01	0.99 ± 0.01
1×2	5–8-1	5.02 ± 3.51	0.21 ± 0.15	0.99 ± 0.01	0.99 ± 0.01	7.59 ± 4.87	0.30 ± 0.19	0.99 ± 0.01	0.99 ± 0.01
1.5×1.5*	**5-18-1**	**1.60 ± 1.48**	**0.07 ± 0.07**	**0.99 ± 0.01**	**0.99 ± 0.01**	**4.42 ± 2.43**	**0.15 ± 0.09**	**0.99 ± 0.01**	**0.99 ± 0.01**
1.5×2	5–16-1	3.45 ± 4.36	0.14 ± 0.18	0.99 ± 0.01	0.99 ± 0.01	5.43 ± 5.59	0.20 ± 0.21	0.99 ± 0.01	0.99 ± 0.01
2×2	5–10-1	3.32 ± 4.34	0.14 ± 0.18	0.99 ± 0.01	0.99 ± 0.01	4.94 ± 5.42	0.18 ± 0.21	0.99 ± 0.01	0.99 ± 0.01

* The bold numbers are the statistical parameters of the best predictive model.

Table 5
Selection the best neuron in MLP model with LM algorithm by application of K-fold cross validation method.

Number of neurons	Train		Test		Total	
	MAPE %	R^2 (−)	MAPE %	R^2 (−)	MAPE %	R^2 (−)
	($\bar{x}$±SD)	($\bar{x}$±SD)	($\bar{x}$±SD)	($\bar{x}$±SD)	($\bar{x}$±SD)	($\bar{x}$±SD)
5	1.3873 ± 0.0911	0.9937 ± 0.0008	1.4055 ± 0.0977	0.9935 ± 0.0009	1.3982 ± 0.0935	0.9936 ± 0.0008
6	1.3357 ± 0.1348	0.9942 ± 0.0011	1.3499 ± 0.1400	0.9941 ± 0.0012	1.3442 ± 0.1367	0.9941 ± 0.0012
7	1.3030 ± 0.1535	0.9945 ± 0.0013	1.3221 ± 0.1539	0.9944 ± 0.0013	1.3145 ± 0.1527	0.9944 ± 0.0013
8	1.2683 ± 0.1750	0.9948 ± 0.0014	1.2822 ± 0.1714	0.9947 ± 0.0014	1.2766 ± 0.1720	0.9947 ± 0.0014
9	1.2108 ± 0.2075	0.9954 ± 0.0015	1.2298 ± 0.2114	0.9953 ± 0.0015	1.2222 ± 0.2091	0.9954 ± 0.0015
10	1.2150 ± 0.2032	0.9955 ± 0.0014	1.2279 ± 0.2073	0.9953 ± 0.0015	1.2228 ± 0.2051	0.9954 ± 0.0014
11	1.1904 ± 0.2267	0.9957 ± 0.0016	1.2068 ± 0.2331	0.9956 ± 0.0016	1.2002 ± 0.2299	0.9956 ± 0.0016
12	1.1828 ± 0.2124	0.9959 ± 0.0014	1.1933 ± 0.2115	0.9958 ± 0.0014	1.1891 ± 0.2110	0.9959 ± 0.0014
13	1.1230 ± 0.2359	0.9961 ± 0.0016	1.1373 ± 0.2406	0.9961 ± 0.0017	1.1316 ± 0.2383	0.9961 ± 0.0016
14	1.1559 ± 0.2281	0.9962 ± 0.0015	1.1700 ± 0.2280	0.9961 ± 0.0015	1.1643 ± 0.2275	0.9961 ± 0.0015
15	1.1440 ± 0.2116	0.9963 ± 0.0013	1.1575 ± 0.2203	0.9962 ± 0.0014	1.1521 ± 0.2163	0.9962 ± 0.0013
16	1.1445 ± 0.2372	0.9963 ± 0.0015	1.1629 ± 0.2399	0.9961 ± 0.0016	1.1556 ± 0.2383	0.9962 ± 0.0016
17	1.1028 ± 0.2283	0.9966 ± 0.0014	1.1159 ± 0.2276	0.9965 ± 0.0015	1.1106 ± 0.2274	0.9965 ± 0.0015
18	1.0991 ± 0.2559	0.9965 ± 0.0015	1.1168 ± 0.2560	0.9965 ± 0.0015	1.1097 ± 0.2554	0.9965 ± 0.0015
19	1.0904 ± 0.2255	0.9967 ± 0.0014	1.1045 ± 0.2297	0.9966 ± 0.0014	1.0988 ± 0.2275	0.9966 ± 0.0014
20*	**1.0286 ± 0.2879**	**0.9971 ± 0.0016**	**1.0470 ± 0.2900**	**0.9970 ± 0.0017**	**1.0397 ± 0.2888**	**0.9970 ± 0.0017**
21	1.1367 ± 0.2467	0.9964 ± 0.0016	1.1521 ± 0.2440	0.9963 ± 0.0016	1.1459 ± 0.2445	0.9963 ± 0.0016
22	1.0907 ± 0.2549	0.9965 ± 0.0016	1.1110 ± 0.2630	0.9964 ± 0.0016	1.1029 ± 0.2591	0.9965 ± 0.0016
23	1.1405 ± 0.2543	0.9965 ± 0.0015	1.1558 ± 0.2574	0.9964 ± 0.0015	1.1497 ± 0.2556	0.9964 ± 0.0015
24	1.0942 ± 0.2470	0.9967 ± 0.0015	1.1065 ± 0.2463	0.9966 ± 0.0016	1.1016 ± 0.2461	0.9966 ± 0.0016
25	1.0958 ± 0.2718	0.9966 ± 0.0016	1.1182 ± 0.2758	0.9965 ± 0.0016	1.1092 ± 0.2739	0.9965 ± 0.0016
26	1.1076 ± 0.2617	0.9966 ± 0.0015	1.1243 ± 0.2636	0.9965 ± 0.0015	1.1176 ± 0.2624	0.9965 ± 0.0015
27	1.0810 ± 0.2615	0.9968 ± 0.0015	1.0962 ± 0.2599	0.9967 ± 0.0015	1.0902 ± 0.2601	0.9968 ± 0.0015
28	1.0580 ± 0.2738	0.9970 ± 0.0015	1.0738 ± 0.2750	0.9970 ± 0.0015	1.0675 ± 0.2742	0.9970 ± 0.0015
29	1.1162 ± 0.2794	0.9965 ± 0.0017	1.1336 ± 0.2853	0.9964 ± 0.0018	1.1266 ± 0.2824	0.9965 ± 0.0017
30	1.1215 ± 0.2789	0.9967 ± 0.0016	1.1388 ± 0.2789	0.9966 ± 0.0017	1.1319 ± 0.2784	0.9966 ± 0.0017

* The bold numbers are the statistical parameters of the best topology.

There is not any similar research about collectors but in other applications, some researchers reported similar results about ANN models. For example, Kalogirou (2006), applied ANN model to estimate the collector performance parameters and reported that this method can use with high precision. Also the authors indicate that the performance of ANN can be improved by more training and use other new and sufficient algorithms.

In a similar study, ANN models (MLP and RBF) were applied to predict the output yield of wheat production (Taki et al., 2018b). The results showed that ANN models can use with high performance to predict the

Table 6
Selection the best neuron in MLP model with BR algorithm by application of K-fold cross validation method.

Number of neurons	Train		Test		Total	
	MAPE (%)	R^2 (−)	MAPE (%)	R^2 (−)	MAPE (%)	R^2 (−)
	($\bar{x}$±SD)	($\bar{x}$±SD)	($\bar{x}$±SD)	($\bar{x}$±SD)	($\bar{x}$±SD)	($\bar{x}$±SD)
5	0.8884 ± 0.1460	0.9976 ± 0.0010	0.8717 ± 0.1504	0.9975 ± 0.0010	0.8664 ± 0.1482	0.9975 ± 0.0010
6	0.6196 ± 0.0913	0.9987 ± 0.0004	0.6328 ± 0.0911	0.9987 ± 0.0004	0.6275 ± 0.0918	0.9987 ± 0.0004
7	0.4546 ± 0.0888	0.9993 ± 0.0003	0.4672 ± 0.0902	0.9993 ± 0.0003	0.4621 ± 0.0894	0.9993 ± 0.0003
8	0.3571 ± 0.0627	0.9996 ± 0.0002	0.3679 ± 0.0636	0.9996 ± 0.0002	0.3636 ± 0.0631	0.9996 ± 0.0002
9	0.3054 ± 0.0523	0.9997 ± 0.0001	0.3161 ± 0.0541	0.9997 ± 0.0001	0.3118 ± 0.0532	0.9997 ± 0.0001
10	0.2627 ± 0.0348	0.9998 ± 0.0001	0.2731 ± 0.0365	0.9998 ± 0.0001	0.2689 ± 0.0356	0.9998 ± 0.0001
11	0.2257 ± 0.0223	0.9998 ± 0.0001	0.2363 ± 0.0232	0.9998 ± 0.0001	0.2321 ± 0.0225	0.9998 ± 0.0001
12	0.2058 ± 0.0184	0.9999 ± 0.0001	0.2160 ± 0.0183	0.9999 ± 0.0001	0.2119 ± 0.0180	0.9999 ± 0.0001
13	0.1882 ± 0.0148	0.9999 ± 0.0001	0.1985 ± 0.0154	0.9999 ± 0.0001	0.1944 ± 0.0148	0.9999 ± 0.0001
14	0.1733 ± 0.0143	0.9999 ± 0.0001	0.1831 ± 0.0144	0.9999 ± 0.0001	0.1792 ± 0.0140	0.9999 ± 0.0001
15	0.1599 ± 0.0116	0.9999 ± 0.0001	0.1697 ± 0.0107	0.9999 ± 0.0001	0.1658 ± 0.0108	0.9999 ± 0.0001
16	0.1482 ± 0.0118	0.9999 ± 0.0001	0.1589 ± 0.0129	0.9999 ± 0.0001	0.1546 ± 0.0121	0.9999 ± 0.0001
17	0.1347 ± 0.0113	0.9999 ± 0.0001	0.1445 ± 0.0116	0.9999 ± 0.0001	0.1406 ± 0.0112	0.9999 ± 0.0001
18	0.1250 ± 0.0131	0.9999 ± 0.0001	0.1349 ± 0.0130	0.9999 ± 0.0001	0.1309 ± 0.0128	0.9999 ± 0.0001
19	0.1169 ± 0.0113	0.9999 ± 0.0001	0.1269 ± 0.0125	0.9999 ± 0.0001	0.1229 ± 0.0117	0.9999 ± 0.0001
20	0.1066 ± 0.0103	0.9999 ± 0.0001	0.1165 ± 0.0115	0.9999 ± 0.0001	0.1126 ± 0.0108	0.9999 ± 0.0001
21	0.1018 ± 0.0109	0.9999 ± 0.0001	0.1111 ± 0.0115	0.9999 ± 0.0001	0.1074 ± 0.0111	0.9999 ± 0.0001
22	0.0990 ± 0.0143	0.9999 ± 0.0001	0.1086 ± 0.0143	0.9999 ± 0.0001	0.1048 ± 0.0142	0.9999 ± 0.0001
23	0.0903 ± 0.0098	0.9999 ± 0.0001	0.1002 ± 0.0113	0.9999 ± 0.0001	0.0963 ± 0.0105	0.9999 ± 0.0001
24	0.0880 ± 0.0112	0.9999 ± 0.0001	0.0982 ± 0.0115	0.9999 ± 0.0001	0.0942 ± 0.0113	0.9999 ± 0.0001
25	0.0804 ± 0.0080	0.9999 ± 0.0001	0.0899 ± 0.0092	0.9999 ± 0.0001	0.0861 ± 0.0085	0.9999 ± 0.0001
26	0.0771 ± 0.0097	0.9999 ± 0.0001	0.0869 ± 0.0115	0.9999 ± 0.0001	0.0830 ± 0.0107	0.9999 ± 0.0001
27*	**0.0552 ± 0.0052**	**0.9999 ± 0.0001**	**0.0648 ± 0.0053**	**0.9999 ± 0.0001**	**0.0610 ± 0.0051**	**0.9999 ± 0.0001**
28	0.0717 ± 0.0092	0.9999 ± 0.0001	0.0812 ± 0.0109	0.9999 ± 0.0001	0.0774 ± 0.0101	0.9999 ± 0.0001
29	0.0672 ± 0.0071	0.9999 ± 0.0001	0.0769 ± 0.0076	0.9999 ± 0.0001	0.0730 ± 0.0073	0.9999 ± 0.0001
30	0.0650 ± 0.0093	0.9999 ± 0.0001	0.0744 ± 0.0850	0.9999 ± 0.0001	0.0706 ± 0.0088	0.9999 ± 0.0001

* The bold numbers are the statistical parameters of the best topology.

Table 7
Selection the best topology between the results of the MLP-LM and MLP-BR models.

Training algorithm	Topology	Statistical parameters (Total phase)			
		MAPE (%) ($\bar{x}$±SD)	RMSE (KJm^{-2} year^{-1}) ($\bar{x}$±SD)	EF (−) ($\bar{x}$±SD)	R^2 (−) ($\bar{x}$±SD)
LM (Levenberg Marquardt)	5–20-1	1.0397 ± 0.2888	25.4883 ± 6.8241	0.9962 ± 0.0020	0.9970 ± 0.0016
BR (Bayesian regularization)	5–27-1	0.0609 ± 0.0050	1.5210 ± 0.1232	0.9999 ± 0.0001	0.9999 ± 0.0001

wheat yield for the next cultivation. In another study, Ghritlahre and Prasad (2018), developed MLP and Multiple Linear Regression (MLR) models to predict the heat transfer of two different types of roughened solar air heaters. The results showed that ANN models with 5-10-1 topology can predict the heat transfer characteristics with high accuracy ($R^2 = 0.9953$) than MLR. In another study, ANN-MLP model was used to predict the performance of solar chimney filled with phase change materials (Fadaei et al., 2018). The results showed that the correlation coefficient between the actual and predicted data was more than 0.99 and also the relative error is less than 3%.

In the second section, all the data based on the Table 2 were used for ANN analysis. In this section the effect of data size can be evaluated. So as the last section, the TanSig transfer function with LM and BR training algorithms and the different number of neurons in hidden layer (1,2,3…,30) were used for ANN modeling. Table 5 shows the results of MLP-LM model with different number of neurons in the hidden layer in train, test and total phases.

The results of Table 6 indicated that, the best topology with highest performance is 5–20-1. Total MAPE and R^2 for this structure are 1.0397 ± 0.2888 and 0.9970 ± 0.0017, respectively. Based on the Table 5, the MAPE of MLP-LM structure in total phase was varied between 1.0397 and 1.3982%. Also, this table show that the data size of training has not a significant effect on total MAPE of MLP-LM structure in this study. So the analysis was repeated for MLP-BR model with same structure of MLP-LM (Table 6). The results of Table 6 show that MAPE and R^2 at total phase for the best topology with MLP-BR structure (5–27-1) are 0.0610 ± 0.0051% and 0.9999 ± 0.0001, respectively. MAPE for different number of neurons in the hidden layer is varied between 0.0610 ± 0.0051 to 0.8664 ± 0.1482%. The results of MLP-BR analysis show that the standard deviation in train, test and total phases is very low compared with the same results of MLP-LM. The MAPE for the best topology (5–27-1) in MLP-BR is more than 16 times lower than the same MAPE for the best topology by MLP-LM (5–20-1). Table 7 shows a brief comparison with all statistical parameters between the best topologies by LM and BR training algorithms.

Fig. 5.A shows Cross-Correlation of predicted and actual values by the best topology (5–27-1) and B: shows the convergence diagram of this topology at train, test and validation phases. Fig. 5A shows that after 677 repetitions, the MSE for train, test and total phases reached to the minimum value and MLP-BR model was learned to predict the output with lowest error. Also the next section (B) shows that this topology can accounted more than 99% of total actual variability in the real data. The correlation coefficient between the actual and predicted data in train, test, validation and total phases are very high. So, this model can show the relation between the inputs and output with high accuracy and can be accepted for experimental applications. Many researchers reported that the ANN model could solve problem equation and predict the results with high accuracy in all aspect of sciences (Elsheikh et al., 2019). Sözen et al. (2008), applied ANN method to evaluate the performance of flat-plate solar collector and reported that the maximum deviation between the actual and predicted data by ANN model was about 2.55%.

3.2. Sensitivity analysis

In the last section, the sensitivity analysis was evaluated for MLP-BR structure. By sensitivity analysis, the share of each inputs on the output can be calculated. Fig. 6 shows the sensitivity analysis for MLP-BR (5–27-1) in this study. As it can be seen, the share of height on the energy gain reduction due to shadow in flat-plate solar collectors, is higher than other parameters. This is similar to the result of mathematical modeling (Farhadi and Taki, 2020). So, finding the best height in all the dimensions and in all the latitudes and tilts, is a main factor for optimization the energy lost due to shadow in flat-plate solar collectors. By the results of this study, engineers can find the energy lost in flat-plate solar collectors in the world and the optimum dimensions and height can be find by ANN model before construction. The authors strongly suggested to adopt the best ANN models for every county based on the local dimensions of flat-plate solar collectors and decrease the energy lost and improve the efficiency of solar collectors.

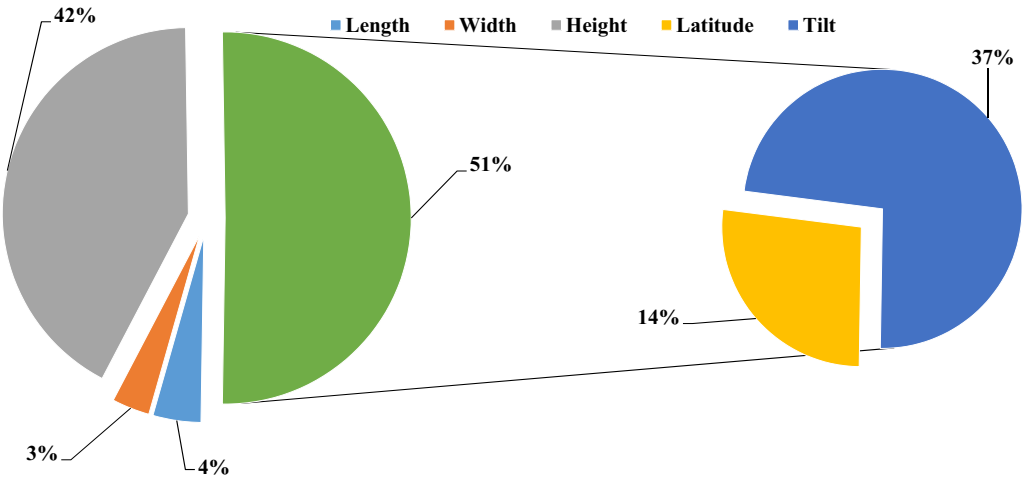

Fig. 6. The sensitivity analysis of the inputs and their effects on the output for MLP-BR with (5–27-1) topology.

4. Conclusion

In this study, ANN-MLP method was developed for modeling the energy gain reduction due to shadow in flat-plate solar collectors. Two training algorithms (LM-BR) with TanSig transfer function and K-fold cross validation method were used for ANN modeling. Four statistical parameters including Root Mean Square Error (RMSE), Mean Absolute Percentage Error (RMSE), Efficiency Factor (EF) and correlation of determination (R^2) were used for evaluate the precision of ANN model. The inputs including Latitude, Length, Width, Height and tilt were extracted from Farhadi and Taki (2020). In this study, two scenarios were evaluated. In the first scenario, the dimensions (Length×Width) were divided into 5 categories including (1×1; 1×1.5; 1×2; 1.5×1.5; 1.5×2 and 2×2) and in the second, all the range of dimensions (Length: 0.5–2.5 and Wight: 0.5–2.5 m) were used in the inputs data. The results showed that MLP-BR has the lowest MAPE and RMSE than MLP-LM in the two scenarios. MAPE for different number of neurons in the hidden layer was varied between 0.0610 ± 0.0051 to 0.8664 ± 0.1482% in the second scenario. Also, the best topology was (5–27-1) that achieved to MAPE and R^2 of 0.0610 ± 0.0051% and 0.9999 ± 0.0001, respectively. The results of sensitivity analysis indicated that height has the biggest effect on the output (42%) followed by tilt (37%) and latitude (14%). The results of this study showed that ANN method can predict the output data with reasonable accuracy and also combination the K-fold cross validation with ANN can increase the reliability of the ANN outputs.

Declaration of Competing Interest

The authors do not have any type of conflict of interest.

Acknowledgement

The authors would like to thank the editor in chief and the anonymous referees for their valuable suggestions and useful comments that improved the paper content substantially. This study was supported by a grant (981/38) from Agricultural Sciences and Natural Resources University of Khuzestan, Iran. The authors are grateful for the support provided by this University.

References

Aidinlou, H.R., Nikbakht, A.M., 2017. Intelligent modeling of thermohydraulic behavior in solar air heaters with artificial neural networks. Neural Comput. & Applic. 31, 3279–3293.

Alonso, J.P., Garcia, M.P., Romera, M.P., Ferre, A., 2012. Performance analysis and neural modeling of a greenhouse integrated photovoltaic system. Renew. Sust. Energ. Rev. 16, 4675–4685.

Al-Waeli, A.H.A., Sopian, K., Yousif, P., 2019. Artificial neural network modeling and analysis of photovoltaic/thermal system based on the experimental study. Energy Convers. Manag. 186, 368–379.

Amini, S., Taki, M., Rohani, A., 2020. Applied improved RBF neural network model for predicting the broiler output energies. Appl. Soft Comput. J. 87, 106006.

Assari, M.R., Basirat Tabrizi, H., Savadkohy, M., 2018. Numerical and experimental study of inlet-outlet locations effect in horizontal storage tank of solar water heater. Sustain. Energy Technol. Assess. 25, 181–190.

Benli, H., 2013. Determination of thermal performance calculation of two different types solar air collectors with the use of artificial neural networks. Int. J. Heat Mass Transf. 60, 1–7.

Çakmak, G., Yıldız, C., 2011. The prediction of seedy grape drying rate using a neural network method. Comput. Electron. Agric. 75 (1), 132–138.

Castañeda-Miranda, A., Castaño, V.M., 2017. Smart frost control in greenhouses by neural networks models. Comput. Electron. Agric. 137, 102–114.

Dimri, N., Tiwari, A., Tiwari, G.N., 2019. An overall exergy analysis of glass-tedlar photovoltaic thermal air collector incorporating thermoelectric cooler: a comparative study using artificial neural networks. Energy Convers. Manag. 195, 1350–1358.

Duffie, J.A., Beckman, W.A., 2013. Solar Engineering of Thermal Processes. New Jersey, John Wiley & Sons, Inc., Hoboken.

Elsheikh, A.H., Abd Elaziz, M., 2018. Review on applications of particle swarm optimization in solar energy systems. Int. J. Environ. Sci. Technol. 16, 1159–1170.

Elsheikh, A.H., Sharshir, S.W., Abd Elaziz, M., Kabeel, A.E., Guilan, W., Haiou, Z., 2019. Modeling of solar energy systems using artificial neural network: a comprehensive review. Sol. 180, 622–639.

Esen, H., Ozgen, F., Esen, M., Sengur, A., 2009. Artificial neural network and wavelet neural network approaches for modelling of a solar air heater. Expert Syst. Appl. 36 (8), 11240–11248.

Esen, H., Esen, M., Ozsolak, O., 2017. Modelling and experimental performance analysis of solar-assisted ground source heat pump system. J. Exp. Theor. Artif. Intell. 29, 1–17.

Fadaei, N., Yan, W.M., Tafarroj, M.M., Kasaeian, A., 2018. The application of artificial neural networks to predict the performance of solar chimney filled with phase change materials. Energy Convers. Manag. 171, 1255–1262.

Farhadi, R., Taki, M., 2020. The energy gain reduction due to shadow inside a flat-plate solar collector. Renew. Energy 147, 730–740.

Fourati, F., 2014. Multiple neural control of a greenhouse. Neurocomputing. 139, 138–144.

Ghritlahre, H.K., Prasad, R.K., 2017. Prediction of thermal performance of unidirectional flow porous bed solar air heater with optimal training function using artificial neural network. Energy Procedia 109, 369–376.

Ghritlahre, H.K., Prasad, R.K., 2018. Prediction of heat transfer of two different types of roughened solar air heater using artificial neural network technique. Therm. Sci. Eng. Prog. 8, 145–153.

Graditi, G., Ferlito, S., Adinolfi, G., Tina, G.M., Ventura, C., 2016. Energy yield estimation of thin-film photovoltaic plants by using physical approach and artificial neural networks. Sol. Energy 130, 232–243.

Hamdan, M.A., Abdelhafez, E.A., Hamdan, A.M., Khalil, R.A.H., 2016. Heat transfer analysis of a flat-plate solar air collector by using an artificial neural network. J. Infrastruct. Syst. 22 (4), 4–14.

Hematian, A., Ajabshirchi, Y., Ranjbar, F., Taki, M., 2021. An experimental analysis of a solar-assisted heat pump (SAHP) system for heating a semisolar greenhouse. Energy Sourr. Part A: Recov. Utiliz. Environ. Effects. 43 1724–174.

Heng, S.Y., Asako, Y., Suwa, T., Nagasaka, K., 2019. Transient thermal prediction methodology for parabolic trough solar collector tube using artificial neural network. Renew. Energy 131, 168–179.

Herez, A., Ramadan, M., Khaled, M., 2018. Review on solar cooker systems: economic and environmental study for different Lebanese scenarios. Renew. Sust. Energ. Rev. 81, 421–432.

Jahangiri Mamouri, S., Bénard, A., 2018. New design approach and implementation of solar water heaters: a case study in Michigan. Sol. Energy 162, 165–177.

Jia, Y., Alva, G., Fang, G., 2019. Development and applications of photovoltaic–thermal systems: a review. Renew. Sust. Energ. Rev. 102, 249–265.

Joshi, S.B., Jani, A.R., 2015. Design, development and testing of a small scale hybrid solar cooker. Sol. Energy 122, 148–155.

Kai, W., Bo, F., Yilin, Z., Qi, X., 2009. The Simulation Research of Solar Assisted Heat Pump System with the Neutral Network. Springer, Berlin Heidelberg, Berlin, Heidelberg, pp. 833–836.

Kalani, H., Sardarabadi, M., Passandideh-Fard, M., 2017. Using artificial neural network models and particle swarm optimization for manner prediction of a photovoltaic thermal nanofluid based collector. Appl. Therm. Eng. 113, 1170–1177.

Kalogirou, S.A., 2006. Prediction of flat-plate collector performance parameters using artificial neural networks. Sol. Energy 80 (3), 248–259.

Kalogirou, S.A., 2014. Solar Energy Engineering: Processes and Systems. Academic Press, California.

Kalogirou, S.A., Panteliou, S., 2000. Thermosiphon solar domestic water heating systems: long-term performance prediction using artificial neural networks. Sol. Energy 69 (2), 163–174.

Kalogirou, S.A., Panteliou, S., Dentsoras, A., 1999. Modeling of solar domestic water heating systems using artificial neural networks. Sol. Energy 65 (6), 335–342.

Khatib, T., Ghareeb, A., Tamimi, M., Jaber, M., Jaradat, S., 2018. A new offline method for extracting I–V characteristic curve for photovoltaic modules using artificial neural networks. Sol. Energy 173, 462–469.

Kumar, K.V., Paradeshi, L., Srinivas, M., Jayaraj, S., 2016. Parametric studies of a simple direct expansion solar assisted heat pump using ANN and GA. Energy Procedia 90, 625–634.

Kurt, H., Atik, K., Özkaymak, M., Recebli, Z., 2008. Thermal performance parameters estimation of hot box type solar cooker by using artificial neural network. Int. J. Therm. Sci. 47 (2), 192–200.

Loni, R., Asli-Ardeh, E.A., Ghobadian, B., Ahmadi, M.H., Bellos, E., 2018. GMDH modeling and experimental investigation of thermal performance enhancement of hemispherical cavity receiver using MWCNT/oil nanofluid. Sol. Energy 171, 790–803.

Mashaly, A.F., Alazba, A., 2015. Comparative investigation of artificial neural network learning algorithms for modeling solar still production. J. Water Reuse Desalinat. 5 (4), 480–493.

Mellit, A., Sağlam, S., Kalogirou, S.A., 2013. Artificial neural network-based model for estimating the produced power of a photovoltaic module. Renew. Energy 60, 71–78.

Mohanraj, M., Jayaraj, S., Muraleedharan, C., 2008. Modeling of a direct expansion solar assisted heat pump using artificial neural networks. Int. J. Green Energy. 5 (6), 520–532.

Mohanraj, M., Belyayev, Y., Jayaraj, S., Kaltayev, A., 2018. Research and developments on solar assisted compression heat pump systems – a comprehensive review (part a: modeling and modifications). Renew. Sust. Energ. Rev. 83, 90–123.

Mostafaeipour, A., Zarezade, M., Goudarzi, H., Rezaei-Shouroki, M., Qolipour, M., 2017. Investigating the factors on using the solar water heaters for dry arid regions: a case study. Renew. Sust. Energ. Rev. 78, 157–166.

Nahar, N.M., Garg, H.P., 1980. Free convection and shading due to gap spacing between an absorber plate and the cover glazing in solar energy flat-plate collectors. Appl. Energy 7, 129–145.

Najafi, G., Ghobadian, B., Tavakoli, T., Buttsworth, D.R., Yusaf, T.F., Faizollahnejad, M., 2009. Performance and exhaust emissions of a gasoline engine with ethanol blended gasoline fuels using artificial neural network. Appl. Energy 86, 630–639.

Nemati, O., Ibarra, L.M.C., Fung, A.S., 2016. Review of computer models of air-based, curtainwall-integrated PV/T collectors. Renew. Sust. Energ. Rev. 63, 102–117.
Nkhonjera, L., Bello-Ochende, T., John, G., King'ondu, C.K., 2017. A review of thermal energy storage designs, heat storage materials and cooking performance of solar cookers with heat storage. Renew. Sust. Energ. Rev. 75, 157–167.
Rai, P., Majumdar, G.C., DasGupta, S., De, S., 2005. Prediction of the viscosity of clarified fruit juice using artificial neural network: a combined effect of concentration and temperature. J. Food Eng. 68 (4), 527–533.
Ranjbar, I., Ajabshirchi, Y., Taki, M., Ghobadifar, A., 2013. Energy consumption and modeling of output energy with MLP Neural Network for dry wheat production in Iran. Elixir Agric. 62, 17949–17953.
Rodriguez, J.D., Perez, A., Lozano, J.A., 2010. A study of cross-validation and bootstrap for accuracy estimation and model selection. Proceeding of the International Joint Conference on Artificial Intelligence. 32, pp. 569–575.
Rohani, A., Taki, M., Abdollahpour, M., 2018. A novel soft computing model (Gaussian process regression with K-fold cross validation) for daily and monthly solar radiation forecasting (part: I). Renew. Energy 115, 411–422.
Rohani, A., Taki, M., Bahrami, G., 2019. Application of artificial intelligence for separation of live and dead rainbow trout fish eggs. Artif. Intell. Agricult. 1, 27–34.
Saravanakumar, P.T., Mayilsamy, K., Sabareesh, V.B., Sabareesan, K.J., 2013. ANN modeling of forced convection solar air heater. In: 2013 International Conference on Current Trends in Engineering and Technology. 1, pp. 57–62.
Souliotis, M., Kalogirou, S., Tripanagnostopoulos, Y., 2009. Modelling of an ICS solar water heater using artificial neural networks and TRNSYS. Renew. Energy 34 (5), 1333–1339.
Sözen, A., Menlik, T., Ünvar, S., 2008. Determination of efficiency of flat-plate solar collectors using neural network approach. Expert Syst. Appl. 35 (4), 1533–1539.
Taki, M., Ajabshirch, Y., Ranjbar, S.F., Rohani, A., Matloobi, M., 2016. Heat transfer and MLP neural network models to predict inside environment variables and energy lost in a semi-solar greenhouse. Energy Build. 110, 34–329.
Taki, M., Abdanan-Mehdizadeh, S., Rohani, A., Rahnama, M., Rahnati-Joneidabad, M., 2018a. Applied machine learning in greenhouse simulation; new application and analysis. Inform. Process. Agricult. 5, 253–268.
Taki, M., Rohani, A., Soheili-Fard, F., Abdeshahi, A., 2018b. Assessment of energy consumption and modeling of output energy for wheat production by neural network (MLP and RBF) and Gaussian process regression (GPR) models. J. Clean. Prod. 172, 3028–3041.
Tomy, A.M., Ahammed, N., Subathra, M.S.P., Asirvatham, L.G., 2016. Analysing the performance of a flat plate solar collector with silver/water nanofluid using artificial neural network. Procedia Comput. Sci. 93, 33–40.
Tripathy, P.P., Kumar, S., 2009. Neural network approach for food temperature prediction during solar drying. Int. J. Therm. Sci. 48 (7), 1452–1459.
Varol, Y., Koca, A., Oztop, H.F., Avci, E., 2010. Forecasting of thermal energy storage performance of phase change material in a solar collector using soft computing techniques. Expert Syst. Appl. 37 (4), 2724–2732.
Yilmaz, C., Koyuncu, I., Alcin, M., Tuna, M., 2019. Artificial neural networks based thermodynamic and economic analysis of a hydrogen production system assisted by geothermal energy on field programmable gate array. Int. J. Hydrog. Energy 44 (33), 17443–17459.